Contrasting multiproxy reconstructions of surface ocean hydrography in the Agulhas Corridor and implications for the Agulhas Leakage during the last 345,000 years

Gema Martínez-Méndez,[1,2] Rainer Zahn,[1,3,4] Ian R. Hall,[5] Frank J. C. Peeters,[6] Leopoldo D. Pena,[7] Isabel Cacho,[8] and César Negre[1,9]

Received 16 October 2009; revised 8 August 2010; accepted 24 August 2010; published 16 December 2010.

[1] Planktonic $\delta^{18}O$ and Mg/Ca-derived sea surface temperature (SST) records from the Agulhas Corridor off South Africa display a progressive increase of SST during glacial periods of the last three climatic cycles. The SST increases of up to 4°C coincide with increased abundance of subtropical planktonic foraminiferal marker species which indicates a progressive warming due to an increased influence of subtropical waters at the core sites. Mg/Ca-derived SST maximizes during glacial maxima and glacial Terminations to values about 2.5°C above full-interglacial SST. The paired planktonic $\delta^{18}O$ and Mg/Ca-derived SST records yield glacial seawater $\delta^{18}O$ anomalies of up to 0.8‰, indicating measurably higher surface salinities during these periods. The SST pattern along our record is markedly different from a $U^{K'}_{37}$-derived SST record at a nearby core location in the Agulhas Corridor that displays SST maxima only during glacial Terminations. Possible explanations are lateral alkenone advection by the vigorous regional ocean currents or the development of SST contrasts during glacials in association with seasonal changes of Agulhas water transports and lateral shifts of the Agulhas retroflection. The different SST reconstructions derived from $U^{K'}_{37}$ and Mg/Ca pose a significant challenge to the interpretation of the proxy records and demonstrate that the reconstruction of the Agulhas Current and interocean salt leakage is not as straightforward as previously suggested.

Citation: Martínez-Méndez, G., R. Zahn, I. R. Hall, F. J. C. Peeters, L. D. Pena, I. Cacho, and C. Negre (2010), Contrasting multiproxy reconstructions of surface ocean hydrography in the Agulhas Corridor and implications for the Agulhas Leakage during the last 345,000 years, *Paleoceanography*, *25*, PA4227, doi:10.1029/2009PA001879.

1. Introduction

[2] The Agulhas Current constitutes the western boundary current of the South Indian Ocean subtropical gyre and transports some 70–78 Sv (1 Sv = 10^6 m^3 s^{-1}) of tropical and subtropical waters along the eastern margin of southern Africa [*Lutjeharms*, 2006]. At the southern tip of Africa, between 15°E and 20°E, the current retroflects and the majority of its waters flow back into the Indian Ocean as the Agulhas Return Current (ARC) [*Feron et al.*, 1992]. Approximately 5–8 Sv [*de Ruijter et al.*, 1999] of warm and salty Indian waters "leak" every year from the Indian into the Atlantic Ocean at the retroflection via the intermittent shedding of Agulhas Rings and formation of Agulhas Filaments [*Lutjeharms*, 1996]. The formation of Agulhas Rings has been linked with the downstream migration along the Agulhas Current of Mozambique Eddies and Natal Pulses [*Lutjeharms*, 1996, 2006] and it is part of the surface return flow that compensates for the export of deep water forming in the subpolar North Atlantic [*Gordon*, 2003]. Hence Agulhas Rings and the ensuing leakage of subtropical water from the Indian Ocean to the Atlantic are involved in the global Thermohaline Circulation (THC).

[3] Despite the Agulhas Current's importance within the global THC and its impact on southeastern African climates [e.g., *Tyson*, 1986] only a few studies have investigated its longer-term history and, in particular, the ensuing interocean water transports [*Chang et al.*, 1999; *Flores et al.*, 1999; *Rau et al.*, 2002; *Peeters et al.*, 2004; *Franzese et al.*, 2006; *Rau et al.*, 2006; *Bard and Rickaby*, 2009; *Franzese et al.*, 2009; *Dickson et al.*, 2010]. Faunal and geochemical evidence from sediment records in the Cape Basin (hereafter CBR, Cape Basin Record) [*Peeters et al.*, 2004] have been used to infer that Agulhas Leakage was maximal during glacial-interglacial transitions, which in conjunction with numerical models

[1]Institut de Ciència i Tecnologia Ambientals, Universitat Autònoma de Barcelona, Bellaterra, Spain.
[2]Now at Center for Marine Environmental Sciences (MARUM), University of Bremen, Bremen, Germany.
[3]Institució Catalana de Recerca i Estudis Avançats, Barcelona, Spain.
[4]Departament de Física, Universitat Autònoma de Barcelona, Bellaterra, Spain.
[5]School of Earth and Ocean Sciences, Cardiff University, Cardiff, UK.
[6]Section Marine Biogeology, Faculty of Earth and Life Sciences, VU University Amsterdam, Amsterdam, Netherlands.
[7]Lamont-Doherty Earth Observatory, Palisades, New York, USA.
[8]GRC Geociències Marines, Departament d'Estratigrafia, Paleontologia i Geociències Marines, Universitat de Barcelona, Barcelona, Spain.
[9]Now at Centre d'Innovació i Formació Ocupacional Santa Coloma, Departament de Treball, Generalitat de Catalunya, Santa Coloma de Gramenet, Spain.

0883-8305/10/2009PA001879

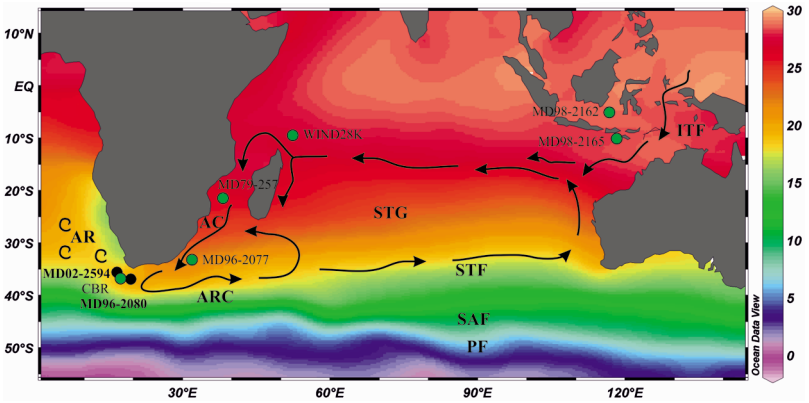

Figure 1. Locations of cores MD02-2594 and MD96-2080 (black dots) and reference sites (green dots) CBR [*Peeters et al.*, 2004], MD96-2077 [*Bard and Rickaby*, 2009], MD79-257 [*Levi et al.*, 2007], WIND28K [*Kiefer et al.*, 2006], MD98-2162 [*Visser et al.*, 2003], and MD98-2165 [*Levi et al.*, 2007]. Labels are Agulhas Current (AC), Agulhas Return Current (ARC), Agulhas Rings (AR), Indonesian Throughflow (ITF), Subtropical Front (STF), Subantarctic Front (SAF), and Polar Front (PF) Subtropical Gyre (STG). Base map illustrates annual mean sea surface temperatures (compiled using the program Ocean Data View (R. Schlitzer, http://gcmd.nasa.gov/records/ODV_AWI.html, 2007)).

suggests a close coupling between the leakage and mode shifts of the Atlantic meridional overturning circulation (AMOC) [*Knorr and Lohmann*, 2003; *Peeters et al.*, 2004; *Knorr and Lohmann*, 2007].

[4] We present new high-resolution planktonic $\delta^{18}O$ and Mg/Ca-derived sea surface temperature (SST) records from two sediment cores in the Atlantic sector of the Agulhas Corridor at the southern tip of Africa (Figure 1). Together with foraminiferal assemblage data the profiles show developments of surface ocean hydrography that are strikingly different from those previously published at a nearby location. Hence our records shed a different light on the interocean water transfer, and potentially its underlying dynamics and they challenge the interpretation of the proxy records and implications previously drawn on the significance of the Agulhas Current and Leakage for the AMOC.

2. Site Location and Materials

[5] We use two sediment cores that were retrieved with the RV *Marion Dufresne* from the Agulhas Corridor at the southern tip of Africa (Figure 1) near the northern limits of the direct influence of warm saline waters drawn from the subtropical gyre of the South Indian Ocean by the Agulhas Current.

[6] Core MD96-2080 (36°19.2′S; 19°28.2′E, 2488 m water depth) was retrieved during the IMAGES II Campaign "NAUSICAA" [*Bertrand et al.*, 1997] and was studied previously by *Rau et al.* [2002, 2006], who established low-resolution benthic stable isotope and foraminiferal assemblage records for the last 850 kyr B.P. A high-resolution study by *Martínez-Méndez et al.* [2008] of the upper 8 m of this core established fine-scale deep water proxy records and detected a hiatus in the upper section of core MD96-2080 that we fill using data from nearby core MD02-2594 (34°42.6′S; 17°20.3′E, 2440 m water depth) (Figure 1). This core was retrieved during RV *Marion Dufresne* cruise MD128 "SWAF" (South West Africa Campaign) [*Giraudeau et al.*, 2003]. These records were spliced together to form a single archive, hereafter referred to as the Agulhas Bank Splice (ABS). Details of the splicing procedure are provided in section 4 and in auxiliary material Text S1.[1]

3. Methods

[7] We have produced multicentennial resolution proxy records of *Globigerina bulloides* stable isotopes and Mg/Ca spanning the past 345 kyr B.P., i.e., back to glacial Termination IV (T-IV, the marine isotope stage (MIS) 10/9 transition). Combining both proxy records allows estimation of the oxygen isotopic composition of seawater ($\delta^{18}O_{sw}$) as an indicator of Sea Surface Salinity (SSS) variations. These records are complemented by planktonic foraminiferal census counts, in a subset of samples from MIS 6 to MIS 5e, permitting the reconstruction of the so-called Agulhas Leakage Fauna (ALF) [*Peeters et al.*, 2004]. *G. bulloides* shell weights are used to evaluate potential influences of carbonate dissolution on the Mg/Ca ratios.

3.1. Planktonic $\delta^{18}O$

[8] Along core MD96-2080 $\delta^{18}O$ measurements were performed at a 1 cm sample interval and only occasionally at 2 cm steps. The higher sedimentation rates at MD02-2594 allowed a reduced sampling step of 2–5 cm while maintaining a similar temporal resolution as in MD96-2080. For $\delta^{18}O$ analysis around 20 individuals of *G. bulloides* were picked from the size fraction 250–315 μm (or subsampled as described below for paired Mg/Ca analyses). Stable isotopes were measured with a ThermoFinnigan MAT 252 mass spectrometer linked online to a single acid bath CarboKiel-II carbonate preparation device. External reproducibility of the analyses was monitored using a laboratory standard (Solnhofen

[1] Auxiliary materials are available in the HTML. doi:10.1029/2009PA001879.

Limestone) yielding 0.08‰ for $\delta^{18}O$. All isotope values are referred to the Vienna Peedee Belemnite scale (VPDB) through calibration to the NBS-19 carbonate standard.

3.2. Planktonic Mg/Ca and Sea Surface Temperature Estimation

[9] Mg/Ca analyses were performed every 2–5 cm in both cores. A total of 70–80 individuals of *G. bulloides* were picked from the size fraction 250–315 μm and the shells gently crushed between two glass plates and homogenized. Approximately 1/3 fraction was separated for stable isotope measurements and the rest used for Mg/Ca analysis. Such paired analyses were performed on all samples from core MD02-2594 that was analyzed at a later stage. In the case of MD96-2080 the majority of the stable isotope analyses were performed before the Mg/Ca analyses as an initial screening to check for fine structure of the record. Mg/Ca analyses were then done subsequently with specimens mostly picked from the same samples. Whenever foraminiferal abundance was low, such as occurred in the lower sections of the records, preference was given to the Mg/Ca analyses and $\delta^{18}O$ analyses were skipped because the resolution of the $\delta^{18}O$ record was already high. In these cases (34 out of a total of 401 measurements) $\delta^{18}O$ and Mg/Ca measurements are not paired. Sample cleaning prior to Mg/Ca analysis employed the oxidative cleaning protocol of *Pena et al.* [2005] that includes steps for clay removal, organic matter oxidation and removal of remaining coatings with a weak acid leaching. Trace element measurements were performed using a Perkin Elmer Elan 6000 Inductively Coupled Plasma Mass Spectrometer (ICP-MS). A high-purity gravimetrically prepared standard solution of known Mg/Ca ratio (2.519 mmol/mol) was measured routinely every four samples, achieving an external reproducibility of 2.474 ± 0.102%. This is equivalent to an uncertainty of ±0.3°C at 24.4°C. To monitor sample cleaning, Mn and Al concentrations [e.g., *Boyle*, 1983; *Boyle and Rosenthal*, 1996; *Barker et al.*, 2003; *Pena et al.*, 2005] were measured in each sample and in protocol blanks that were routinely run between samples. Based on this procedure we eliminated four samples out of a total of 401 from the data set. Additional replicates using both the oxidative and full reductive cleaning protocol were performed in selected samples recording maximum Mg/Ca ratios (i.e., deglacial samples, see Figure 3) and results confirmed the reliability of the reconstruction and absence of contamination by oxides or other diagenetic minerals [*Pena et al.*, 2005]. Mg/Ca ratios were converted to SST estimates using the *G. bulloides* based calibration of *Mashiotta et al.* [1999]. Standard errors of this SST calibration are ±0.8°C.

3.3. Seawater Oxygen Isotope Reconstruction ($\delta^{18}O_{sw}$)

[10] The paired planktonic foraminiferal $\delta^{18}O$ and Mg/Ca-derived SST were used to estimate the oxygen isotopic composition of seawater ($\delta^{18}O_{sw}$) as an indicator of past salinity changes. This provides an additional constraint for the paleohydrographic assessment of local surface waters. Before computing $\delta^{18}O_{sw}$ we removed ice-volume signals by subtracting the mean-ocean $\delta^{18}O_{sw}$ record of *Waelbroeck et al.* [2002] from the ABS planktonic $\delta^{18}O$ record. For the MIS 2–3 section we used the higher resolved sea level record of *Siddall et al.* [2003] that we converted to $\delta^{18}O_{sw}$ applying a $\delta^{18}O_{sw}$: sea level slope of 0.008‰/m [*Schrag et al.*, 2002]. The global $\delta^{18}O_{sw}$ records were synchronized with our planktonic $\delta^{18}O$ record by optimizing their graphical fit, i.e., they were tuned to our age scale. This was done to minimize stratigraphic misfits between the global $\delta^{18}O_{sw}$ and our local records that would potentially generate artifacts in the computed local $\delta^{18}O_{sw}$ record. To derive the local $\delta^{18}O_{sw}$, we employed the paleotemperature equation that *Bemis et al.* [2002] established for *Orbulina universa* under low-light conditions. This equation also represents the isotopic composition of the encrusted variety of *G. bulloides* in the Santa Barbara Basin [*Bemis et al.*, 2002]. We report the local $\delta^{18}O_{sw}$ anomaly relative to the late Holocene ($\Delta\delta^{18}O_{sw}$; Figure 4b), converted to the VSMOW scale by adding 0.27 [*Hut*, 1987]. Using the late Holocene (0–5 kyr B.P.) planktonic $\delta^{18}O$ and SST of our ABS record the paleotemperature equation yields a $\delta^{18}O_{sw}$ of 0.38‰ VSMOW which is consistent with the modern surface $\delta^{18}O_{sw}$ of 0.48 ± 0.08‰ VSMOW in the region [*Bigg and Rohling*, 2000; G. A. Schmidt et al., Global seawater oxygen-18 database, 1999; available at http://data.giss.nasa.gov/o18data]. The warm water paleotemperature equation of *Bemis et al.* [1998] that was developed from culturing *G. bulloides* yields a late Holocene $\delta^{18}O_{sw}$ of 1.1‰ VSMOW, more than twice the modern observed value in the region and hence does not seem to represent conditions at our core locations.

3.4. Foraminiferal Census Counts, Agulhas Leakage Fauna

[11] Foraminiferal census counts were performed on a subset of 25 samples from MIS 6 to 5, i.e., from 424–201 cm, to obtain the so-called Agulhas Leakage Fauna index (ALF index) [*Peeters et al.*, 2004], which is considered to reflect the intensity of past Indian-Atlantic water exchange via Agulhas Leakage. This includes the species *Pulleniatina obliquiloculata, Globigerinita glutinata, Hastigerina pelagica, Globorotalia menardii, Globigerinoides sacculifer, Globigerinella siphonifera, Globigerinoides ruber, Orbulina universa, Globoquadrina hexagona* and *Globorotalia scitula*. The ALF index is calculated as the sum of the relative contribution of these species to the total planktonic foraminiferal assemblage [*Peeters et al.*, 2004].

3.5. Planktonic Shell Weights

[12] To check for possible dissolution affects that can alter the Mg/Ca ratios, we determined shell weights of *G. bulloides*. A total of 70–80 individuals that were picked from the size fraction 250–315 μm for stable isotope and trace element analyses were weighed prior to analysis using a microbalance (0.1 μg). The total weight was divided by the number of individuals to obtain a weight estimate for individual shells.

4. Age Model and Construction of the Composite Agulhas Bank Splice Record

[13] The age model we use for core MD96-2080 is that presented previously by *Martínez-Méndez et al.* [2008]. Briefly, it was developed using a combination of radiocarbon dating and graphical correlation of the benthic $\delta^{18}O$ record

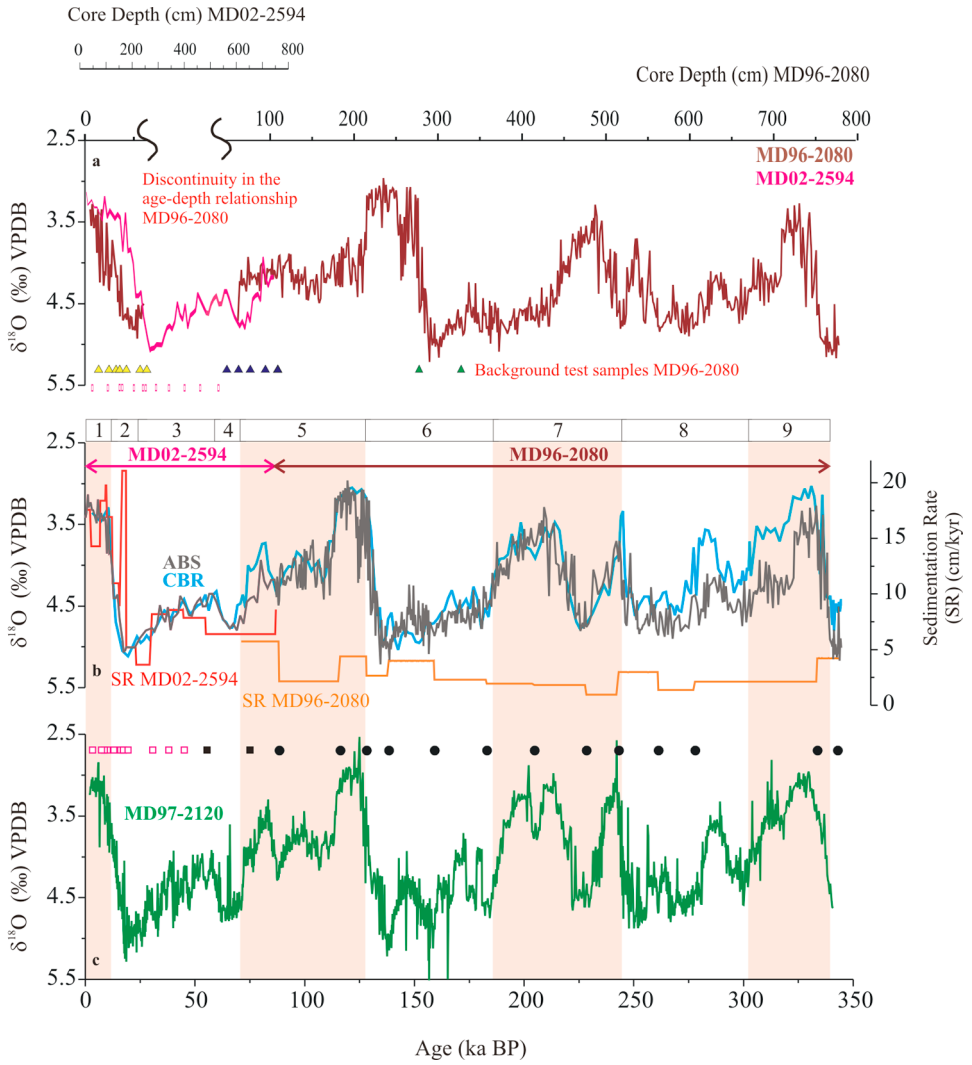

Figure 2. Construction of the "Agulhas Bank Splice" (ABS) record and age model. (a) Benthic $\delta^{18}O$ record of core MD96-2080 (brown) along core depth. Yellow triangles indicate positions of ^{14}C-AMS dates used for age modeling. Blue triangles show the positions of the ^{14}C-AMS samples that indicated the presence of a hiatus (see *Martínez-Méndez et al.* [2008] for details). Green triangles show samples used to indicate background levels in the accelerator mass spectrometer. The benthic $\delta^{18}O$ profile of core MD02-2594 (pink, depth scale indicated separately) is used to fill the hiatus in the upper section of MD96-2080. Pink bars at bottom indicate position of ^{14}C-AMS dates in MD02-2594. (b) Benthic $\delta^{18}O$ of the composite ABS record (gray). The composite CBR profile (blue) [*Peeters et al.*, 2004] is shown on a revised age scale for comparison with the ABS record. Sedimentation rates (cm/kyr scale on right) along the ABS record are shown in red (MD02-2594) and orange (MD96-2080). Top bar gives marine isotope stages. (c) Benthic $\delta^{18}O$ record of core MD97-2120 [*Pahnke and Zahn*, 2005] that has been used for stratigraphic reference to fine-tune the age model of the ABS record. Pink boxes mark ^{14}C-AMS dates for MD02-2594; black boxes and circles denote tie points used to maximize the stratigraphic fit of benthic $\delta^{18}O$ of MD02-2594 and MD96-2080 with that of MD97-2120. Vertical shading highlights interglacials.

with that of core MD97-2120 from Chatham Rise in the southwest Pacific (45°32′S, 174°57′E) [*Pahnke et al.*, 2003; *Pahnke and Zahn*, 2005] (Figure 2). The age model for core MD02-2594 was derived following the same procedure. All radiocarbon analyses were performed on monospecific planktonic foraminiferal samples (*Globorotalia inflata*). The radiocarbon measurements on core MD02-2594 were carried out at the National Ocean Science Accelerator Mass Spectrometry facility at the Woods Hole Oceanographic Institution. Conversion from radiocarbon to calendar age was achieved applying a marine reservoir age R(t) of 615 ± 52 years [*Southon et al.*, 2002] and using the calibration routine of *Fairbanks et al.* [2005] and R. G. Fairbanks et al. (Radiocarbon age to calendar age conversion, 2007; available at http://

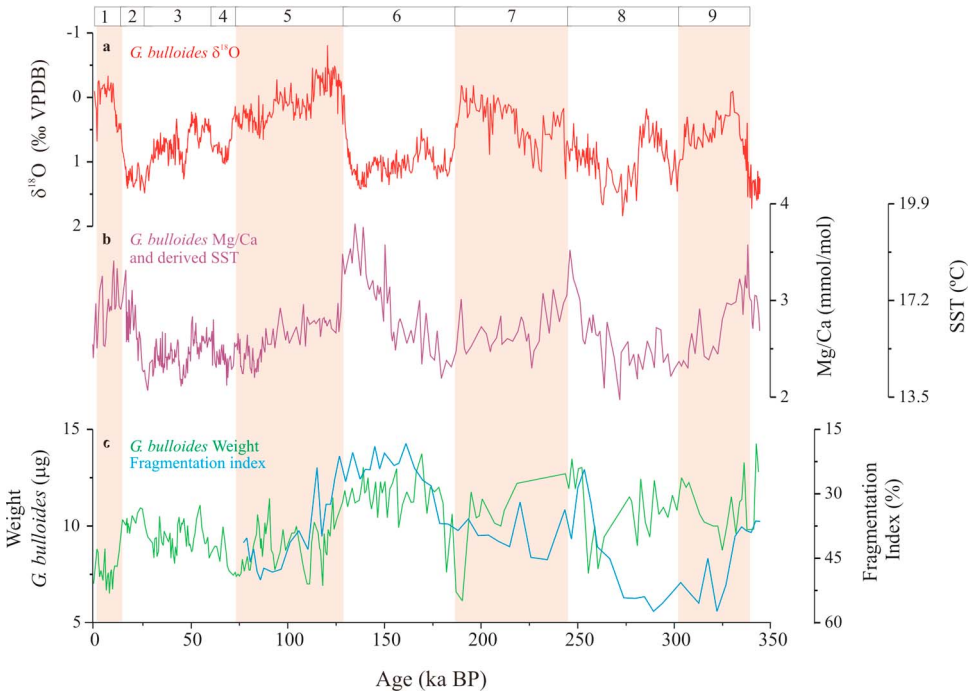

Figure 3. Planktonic profiles along the ABS record. (a) Planktonic $\delta^{18}O$ record of *G. bulloides*. (b) Planktonic Mg/Ca record of *G. bulloides*. Outer scale gives sea surface temperature (°C) derived using the calibration of *Mashiotta et al.* [1999]. (c) Records of *G. bulloides* shell weight (green, this study) (μm) and planktonic foraminifera Fragmentation Index (blue) (FI %, MD96-2080 only [*Rau et al.* 2002]). Top bar displays marine isotope stages. Vertical shading highlights interglacials.

radiocarbon.ldeo.columbia.edu/research/radcarbcal.htm). Details of the splicing procedure between MD02-2594 and MD96-2080 are described in auxiliary material Text S1. In summary, we determined the best fit between MD96-2080 and MD02-2594 by comparing the benthic [*Martínez-Méndez et al.*, 2008, 2009] and planktonic $\delta^{18}O$ and $\delta^{13}C$, planktonic Mg/Ca and $\overline{SS}$ records [*Martínez-Méndez et al.*, 2008; *Negre et al.*, 2010] of both cores. Differences in amplitude and structure of the planktonic and benthic $\delta^{18}O$ [*Martínez-Méndez et al.*, 2008] records in T-I between both cores (Figure 2 and auxiliary material Text S1) we assign to sediment disturbance in the upper part of core MD96-2080 that has also been noted previously [*Bertrand et al.*, 1997]. This potentially allowed mixing of Holocene and LGM sediments hence causing different $\delta^{18}O$ amplitudes and offset structures in both records.

[14] The age model for the ABS record yields sedimentation rates of between 2 and 21 cm/kyr (Figure 2). Maximum rates are recorded around T-I and for the Holocene while minima occur during MIS 7. Our data produces continuous records of *G. bulloides* $\delta^{18}O$ and Mg/Ca back to 345 kyr B.P. at mean time steps $\pm 1\sigma$ of 438 ± 264 yr ($\delta^{18}O$) and 873 ± 783 yr (Mg/Ca).

5. Results

5.1. Planktonic $\delta^{18}O$

[15] Planktonic $\delta^{18}O$ shows orbital scale modulation with glacial-interglacial amplitudes of 1.60 to 1.90‰ (Figure 3a), exceeding coeval $\delta^{18}O$ variations related to ice volume changes by some 0.4 to 0.7‰ [e.g., *Waelbroeck et al.*, 2002]. Only T-III displays a $\delta^{18}O$ amplitude of 0.89‰, virtually identical to the ice-volume effect of this transition. Superimposed on the orbital modulation is a fine-scale structure that alludes to suborbital variability of surface water hydrography. We also note the reduced modulation of the $\delta^{18}O$ profile prior to 200 ka, i.e., in MIS 7–9.

5.2. Mg/Ca-Derived SST

[16] The SST variations inferred from the ABS *G. bulloides* Mg/Ca record (Figures 3b and 4a) display glacial warming's that appear to develop gradually over the course of multiple millennia during MIS 2, 6 and 8. During these stages SST increases progressively from 14 to 15°C during the early to midglacial periods to peak maximum SST above 17–18°C that are reached up to 8 kyr before the onset of glacial Terminations (Figures 3b and 4a). In the case of T-II and T-III, the elevated SST abruptly cool by around 2.5°C as full-interglacial conditions of MIS 5e and 7e are reached while the SST decrease at the end of T-I is less clearly developed (Figures 3b and 4a). Although, our records only marginally extend into MIS 10, elevated Mg/Ca values and hence high SST at the base of the records suggest a similar development during T-IV (Figures 3b and 4a).

5.3. Seawater Oxygen Isotopic Composition ($\delta^{18}O_{sw}$)

[17] The $\Delta\delta^{18}O_{sw}$ record (Figure 4b) displays positive anomalies of 0.5–0.7‰ during MIS 2 and 6 and of about

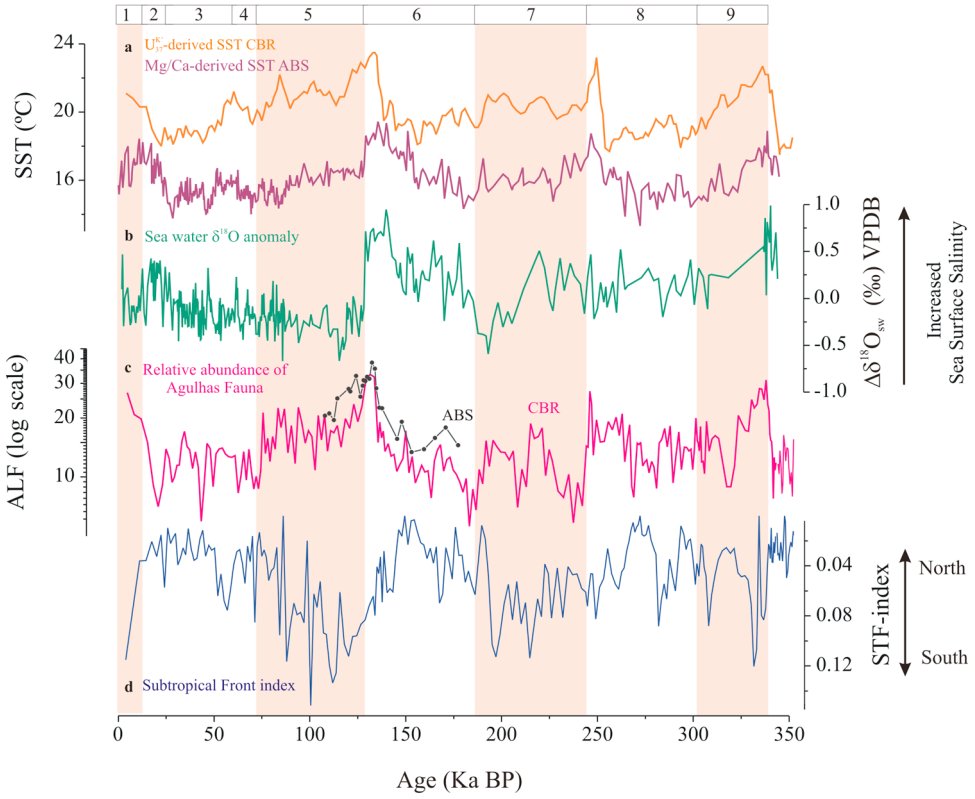

Figure 4. Planktonic records from the Agulhas Corridor. (a) Mg/Ca-derived SST record along ABS (purple, this study) and $U^{K'}_{37}$-derived SST record along CBR (orange) [*Schneider et al.*, 1999; *Peeters et al.*, 2004]. (b) Local seawater δ^{18}O anomaly relative to late Holocene ($\Delta\delta^{18}O_{sw}$) derived from planktonic δ^{18}O (see Figure 3a) and Mg/Ca-derived SST. (c) Abundance of Agulhas Leakage Fauna (ALF) along CBR (pink) [*Peeters et al.*, 2004] and in MIS 6 to 5e of the ABS record (gray dotted). Logarithmic scale was chosen to graphically enhance the good correlation with the Mg/Ca-derived SST and computed $\Delta\delta^{18}O_{sw}$ record. (d) Subtropical Front (STF) faunal index along CBR used as an indicator of latitudinal shifts of the STF [*Peeters et al.*, 2004]. Top bar displays marine isotope stages. Vertical shading highlights interglacials.

1‰ at T-IV, indicating increased SSS during these periods. The SSS anomalies mimic the structure of the SST record in that they built up gradually over the course of several millennia during glacial periods and transgress into the glacial Terminations T-I, T-II and T-IV. They subsequently decrease as full-interglacials are reached. MIS 8 appears to be exceptional as $\Delta\delta^{18}O_{sw}$ remain at levels similar to MIS 9 and the early parts of MIS 7 with only some hint of elevated values during T-III.

5.4. Foraminiferal Census Counts, Agulhas Leakage Fauna

[18] The ALF section that we generated for MIS 6 to MIS 5e (Figure 4c) mimics the SST and SSS developments (Figure 4) as it also displays a progressive increase across MIS 6 and a subsequent abrupt decrease when entering MIS 5e. Plotting the ALF profile on a logarithmic scale to enhance readability of the data for lower abundance variations of the ALF brings out particularly well the trend in the ALF record that follows the shift in SST and SSS. The standard error of ALF percentage is smaller at lower (<20%) than at higher values (>30%), so the logarithmic scaling highlights the low-abundance sections of the record with less standard error.

5.5. Planktonic Shell Weights

[19] *G. bulloides* shells weights vary between 6 and 14 μg with higher values typically observed during glacial periods (Figure 3c). The shell weight record is presented together with the Fragmentation Index (FI) record generated for MD96-2080 (lower part of our spliced ABS) by *Rau et al.* [2002] (Figure 3c). Both records correlate during MIS 5 and 6 with higher shell weights and low FI during MIS 6 indicating better foraminiferal preservation. This correlation is lost down-core, however, particularly during MIS 8-MIS 9 where high values of the FI correspond with high shell weights; hence, the two dissolution proxies provide opposing information in this section.

6. Discussion

6.1. Reliability of the Mg/Ca Record as SST Recorder

[20] Our Mg/Ca record displays a progressive increase of values in the glacial sections indicating increasing SST during

glacial periods. These SST patterns are markedly different from those seen in SST records at other core sites in the region [*Peeters et al.*, 2004; *Cortese et al.*, 2007; *Bard and Rickaby*, 2009]. This can raise concerns about the reliability of the Mg/Ca data and warrants a closer assessment of whether secondary processes biased the Mg/Ca ratios, such as contamination with clays, Mn-rich phases related to secondary carbonate overgrowth [e.g., *Barker et al.*, 2003; *Pena et al.*, 2005] or postdepositional carbonate dissolution [e.g., *Rosenthal et al.*, 2000; *Regenberg et al.*, 2006]. Changes in the salinity of the ambient seawater may likewise influence the Mg/Ca ratios of planktonic foraminifera [*Nürnberg et al.*, 1996; *Ferguson et al.*, 2008; *Groeneveld et al.*, 2008; *Kısakürek et al.*, 2008; *Dueñas-Bohórquez et al.*, 2009; *Sadekov et al.*, 2009].

[21] Postdepositional contamination by clays [e.g., *Barker et al.*, 2003] and/or secondary carbonate overgrowth [e.g., *Pena et al.*, 2005] can be detected by high Al/Ca and Mn/Ca ratios, respectively. The majority of Al/Ca ratios in our sample solutions were at the detection limit of the ICP-MS (4 ppb for Al), only three samples out of 401 yielded Al/Ca values above 200 μmol/mol and were neglected (see section 3). Thus, Mg/Ca alteration by clay contamination can be ruled out. Mn/Ca ratios of our samples remained below the 100–150 μmol/mol limit that is commonly used as the threshold for indicating contamination by Mn-rich overgrowths [*Boyle*, 1983; *Boyle and Rosenthal*, 1996] and only one sample displaying Mn/Ca ratios between 100 and 110 μmol/mol correlated with an elevated Mg/Ca ratio and was discarded. Replicate Mg/Ca analyses using different cleaning protocols (see section 3) yielded consistent results also arguing against contaminant phases.

[22] Carbonate dissolution may affect foraminiferal Mg/Ca ratios as dissolution primarily removes the high-Mg carbonate phases [e.g., *Rosenthal et al.*, 2000]. The cores we used are at around 2500 m water depth and remained above the regional sedimentary calcite lysocline that shifted between 4000 m today and 3500 m during glacials [*Volbers and Henrich*, 2002, 2004]. Therefore we can confidently rule out an influence of carbonate dissolution on Mg/Ca ratios at the sites. This is confirmed by the shell weight distribution of *G. bulloides* along the ABS record, as well as the foraminiferal FI of *Rau et al.* [2002] along MD96-2080 (Figure 3c) that do not correlate with our Mg/Ca and inferred SST records (Figure 3). Only the Mg/Ca decrease at the onset of MIS 5 coincides with decreasing shell weights and an increasing foraminiferal FI which might indicate an influence of carbonate dissolution on shell chemistry which would cause a SST underestimation during MIS 5. However, we note that Mg/Ca-derived SST for most of MIS 5 is consistent with late Holocene and modern SST at this location (see also section 6.2) hence arguing against an influence of carbonate dissolution on Mg/Ca.

[23] Ambient seawater salinity can affect planktonic Mg/Ca ratios in highly evaporative environments [*Ferguson et al.*, 2008] and laboratory culture studies show Mg/Ca increases in selected planktonic foraminifera of 4–7% per psu of salinity increase [*Nürnberg et al.*, 1996; *Lea et al.*, 1999; *Dueñas-Bohórquez et al.*, 2009; *Sadekov et al.*, 2009]. We note that none of these studies specifically monitored possible salinity affects on Mg/Ca ratios in *G. bulloides* but if we use a sensitivity of the SST estimates of 0.8°C per 1 psu salinity change [*Sadekov et al.*, 2009] then a 1 psu ice volume induced SSS increase for MIS 2, 6 and 8 would reduce the SST anomalies recorded in our record from 4.0–5.2°C to 3.2–4.4°C. Assuming a similar magnitude increase in salinity due to an enhanced influence of saline subtropical waters at our core sites during these intervals then the SST anomaly is reduced to 2.5–3.7°C. This suggests that while, in the worst case, the absolute SST estimates may be overestimated by up to 40%, the development of a warm glacial SST anomaly remains a persistent feature.

[24] Accepting the Mg/Ca based SST estimates as correct we derive $\delta^{18}O_{sw}$ as a first order salinity estimation. Inserting the $\delta^{18}O_{sw}$ values into a low-latitude $\delta^{18}O_{sw}$/S relationship (0–18°S; $S = 35.08973 + 0.723 \cdot \delta^{18}O_{sw}$, $1\sigma = \pm 0.62$, n = 78; data source: Schmidt et al. (1999)) that is representative of the subtropical waters carried by the Agulhas Current we derive a SSS anomaly of 1.2–1.5 (including ice volume effects on SSS) for late glacial stages of MIS 2, 6 and 10 and the subsequent Terminations.

6.2. Glacial Surface Water Hydrography in the Agulhas Corridor

[25] The observation of warm SST and elevated $\Delta\delta^{18}O_{sw}$ at our core sites during MIS 2, 6, and 8 (Figure 4b) is suggestive of a more pronounced influence of warm saline Agulhas waters at our core sites. A similar development is suggested for MIS 10 as we also observed elevated SST and $\Delta\delta^{18}O_{sw}$ values around T-IV. This SST pattern is strikingly different from biomarker ($U^{K'}_{37}$) derived SST at a nearby location that shows maximum values only during glacial Terminations (Figure 4a) [*Schneider et al.*, 1999; *Peeters et al.*, 2004] while during glacial periods the $U^{K'}_{37}$-derived SST is decreased which is contrasted by the warming trend seen in our Mg/Ca-derived SST record. One possible explanation for the different SST patterns is that the foraminiferal species we used for Mg/Ca analysis (*G. bulloides*) is not a type subtropical species and hence its Mg/Ca (and $\delta^{18}O$) values may represent the mixing of Agulhas waters with South Atlantic waters. The alkenone producers, on the other hand, may be more closely linked with the subtropical waters of the Agulhas Current which is supported by the close correlation between the ALF percentage and $U^{K'}_{37}$-derived SST records at the nearby CBR location [*Peeters et al.*, 2004]. Another explanation for the different SST reconstructions is differences in the living habitats and growth seasons of the $U^{K'}_{37}$ producers and *G. bulloides* as the Mg/Ca signal carrier [e.g., *Bard*, 2001; *Saher et al.*, 2009]. *G. bulloides* typically calcifies in the upper 50–100 m of the water column [*Niebler et al.*, 1999], prefers nutrient-rich environments such as upwelling regimes, and in the midlatitudes (30°–40°N) has been shown to record winter (February–March) SST [*Elderfield and Ganssen*, 2000; *Ganssen and Kroon*, 2000; *Fraile et al.*, 2009]. SST derived from Mg/Ca of *G. bulloides*, therefore, is more likely to reflect the cold end-member of the seasonal temperature cycle. This is supported by the interglacial Mg/Ca-derived SST in our ABS record that correlates well with austral winter SST at our core sites today. $U^{K'}_{37}$ measurements in seafloor sediments, on the other hand, can also be offset from observed SST due to seasonality in alkenone export production, growth rate variations of the

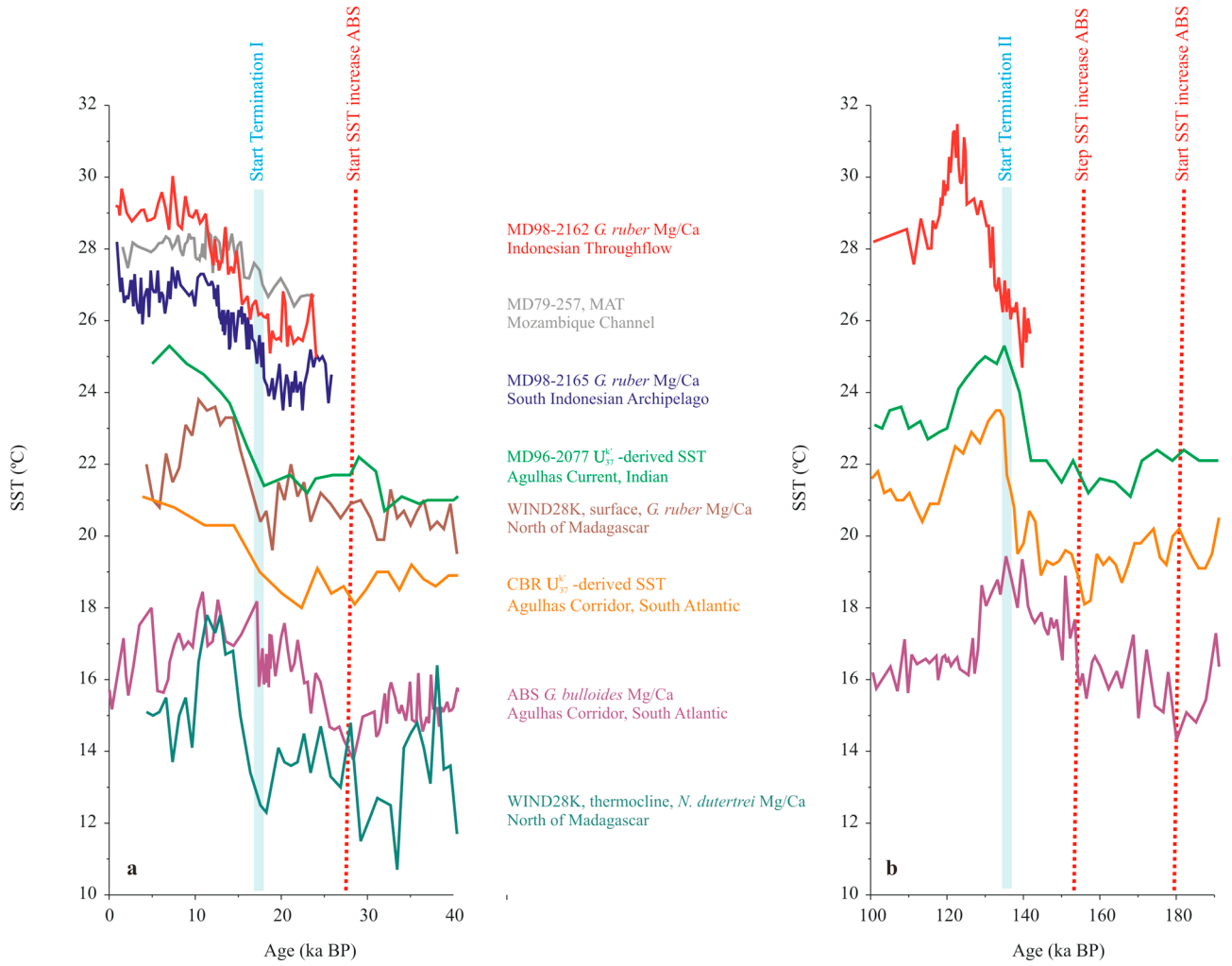

Figure 5. Comparison of the ABS SST record with SST records from core sites in the Indian Ocean (see Figure 1 for core location). (a) MIS 1–3, (b) MIS 5e–6. Core sites and methodologies used to derive SST are as follows: ABS, Mg/Ca in *Globigerina bulloides*, this study; CBR, Atlantic sector of Agulhas Corridor, $U^{K'}_{37}$ index [*Schneider et al.*, 1999; *Peeters et al.*, 2004]; MD96-2077, Indian sector of Agulhas Corridor, $U^{K'}_{37}$ index [*Bard and Rickaby*, 2009]; WIND28K, western tropical Indian, Mg/Ca in *Globigerinoides ruber* (surface dweller) and *Neogloboquadrina dutertrei* (thermocline dweller) [*Kiefer et al.*, 2006]; MD98-2165, south Indonesian archipelago, Mg/Ca in *G. ruber;* MD79-257, Mozambique Channel, foraminifera transfer function using the modern analog technique (MAT) [*Levi et al.*, 2007]; MD98-2162, Indonesian throughflow, Mg/Ca in *G. ruber* [*Visser et al.*, 2003]. SST profiles are shown on their published age scales. The δ^{18}O records of the cores are compiled in Figure S3 in auxiliary material Text S2 for inspection of stratigraphic synchrony.

alkenone producers or postdepositional alkenone degradation [*Sikes et al.*, 2005; *Conte et al.*, 2006; *Prahl et al.*, 2006] or possibly alkenone resuspension at the seafloor and subsequent lateral transportation [*Mollenhauer et al.*, 2003]. We do not have independent controls to assess if any of these factors impacted the $U^{K'}_{37}$-derived SST record and therefore in our further interpretation of $U^{K'}_{37}$- and Mg/Ca-derived SST we take both records at face value.

6.3. Tracing the Signal of Agulhas Waters Upstream

[26] In order to place our records into a paleoceanographic framework of profiles from the wider Indian Ocean we compare our Mg/Ca-derived SST with SST records that were obtained at upstream locations along the Agulhas Current and in other more distant regions that are considered to also have an influence on the current (Figures 1 and 5). Mg/Ca-derived SST records from the Indonesian Throughflow (ITF) region [*Visser et al.*, 2003] and immediately south of Indonesia [*Levi et al.*, 2007] indicate a temperature increase of about 4°C in the course of the last two glacial-to-interglacial transitions. Major steps in the ITF SST record are centered on mid-T-I and T-II and overlap with SST maxima in the ABS record but neither records show the early progressive warming observed in our profile. Mg/Ca-derived temperature records of surface

and thermocline dwelling planktonic foraminifera north of Madagascar [*Kiefer et al.*, 2006] display SST maxima during T-I that are coeval with elevated SST in our record, while, again, the onset of the SST occurs some 10 kyr after the initial SST increase in ABS (Figure 5). Modern analog technique (MAT) SST data from a core site in the Mozambique Channel [*Levi et al.*, 2007] display a 3°C warming during T-I. This record also appears to show an early warming commencing at 21 ka but its stratigraphic reach does not extend beyond 24 ka hindering a detailed comparison with the SST increase in ABS during MIS 2 into the Holocene.

[27] Further to the south, a $U^{K'}_{37}$-derived SST profile from the southeast African margin [*Bard and Rickaby*, 2009] likewise displays maximum SST during glacial Terminations that overlap with the later parts of the SST maxima in our record while a warming as early as in our Mg/Ca derived record is not seen (Figure 5).

[28] While based on different proxies and/or species, these comparisons highlight the distinctive nature of our SST record in that none of the Indian Ocean SST records display warming trends that commence during early or midglacial stages. This suggests the possibility that the Mg/Ca-derived SST variations seen in our record, and the SST offset pattern between our record and $U^{K'}_{37}$-derived SST profiles at nearby core sites, reflect processes that impact the circulation dynamics in the Agulhas Corridor as glacial conditions intensified and then reverted to warmer interglacial conditions.

6.4. Driving Mechanisms

[29] The two primary mechanisms which exert control on the circulation of subtropical waters in the Agulhas Corridor are the strength of the Agulhas Current and the position of the Subtropical Front (STF). Both components operate in concert as the strength of the southward transport of subtropical waters in the Agulhas Current and the position of the STF are both linked with the regional wind field [*Matano et al.*, 1999]. Northward migrations of the STF during glacials are indicated by a range of faunal and geochemical data [*Brathauer and Abelmann*, 1999; *Rau et al.*, 2002; *Gersonde et al.*, 2003; *Peeters et al.*, 2004; *Gersonde et al.*, 2005; *Bard and Rickaby*, 2009] and are diagnostic of a shift of the zero wind stress curl to a location closer to or over the African continent. Under such atmospheric configuration the Agulhas Current should have been weaker [*Lutjeharms*, 2006] and the Agulhas Leakage stronger [*van Sebille et al.*, 2009]. The progressive SST and $\Delta\delta^{18}O_{sw}$ (hence salinity) increases seen in the glacial sections of our records are consistent with an increased influence of subtropical Agulhas water at our sites and a strengthened Agulhas Leakage in the wake of a westward shifted Agulhas retroflection. This, however, is in conflict with the $U^{K'}_{37}$-derived SST record at the nearby CBR location that displays maximum SST during the glacial Terminations while glacial SST are reduced. If indeed the maximum SST that is recorded in both ($U^{K'}_{37}$, Mg/Ca) profiles during the glacial Terminations indicates maximum Agulhas Leakage during the Terminations, this then leaves us to conjecture that the offset SST pattern during glacial periods reflects seasonality of the surface hydrography corresponding to the preferred growth season of the alkenone producers and *G. bulloides* as the Mg/Ca signal carrier. Satellite altimetry data indicate seasonal variability of the position of the Agulhas retroflection such that the retroflection is shifted westward during austral winter [*Matano et al.*, 1998]. Considering a preferred growth season of *G. bulloides* in winter suggests that the Mg/Ca-derived SST would record a stronger influence of Agulhas water during winter while $U^{K'}_{37}$-derived SST would record the summer mode of the Indian-Atlantic connection with a weaker leakage. Provenance studies, using strontium isotope patterns in sediments underlying the flow path of the Agulhas Current and Retroflection [*Franzese et al.*, 2006, 2009] suggest that the mean position of the retroflection under glacial conditions did not deviate much from its modern position. If indeed the mean position of the retroflection was the same during glacial periods this suggests a possibility that a seasonal east-west migration of the retroflection similar to today may have impacted the SST at our and the CBR core locations hence generating the different SST patterns.

[30] The progressive SST and $\Delta\delta^{18}O_{sw}$ increases in ABS during early MIS 6 and 8 are coincident with a northward migration of the STF as indicated in the planktonic foraminiferal STF index record at the CBR location [*Peeters et al.*, 2004] (Figure 4d). An altered circulation dynamics in the Agulhas Corridor due to the northward migration of the STF may have contributed to the offset patterns between the different SST reconstructions, but this cannot be assessed on the basis of the proxy records alone. Ocean models that resolve the Agulhas Current and retroflection at the mesoscale [e.g., *Biastoch et al.*, 2008, 2009] should be able to test the dynamics of the circulation in the Agulhas Corridor as the wind fields shifted away from their modern configuration. Such numerical experiments will also help to gain fuller insight into the significance of such changes for the interocean water transport and salt leakage from the Indian Ocean into the Atlantic.

7. Conclusions

[31] Planktonic foraminiferal $\delta^{18}O$ and Mg/Ca profiles are presented along a composite marine record (Agulhas Bank Splice, ABS) from the Atlantic sector of the Agulhas Corridor at the southern tip of Africa. The records show systematic variability of the surface ocean conditions during the past three glacial-interglacial cycles in that Mg/Ca-derived SST displays progressive warming during glacial periods. Maximum SST levels were reached well before and during glacial Terminations I to III and a similar development is also suggested for T-IV. Combining $\delta^{18}O$ and Mg/Ca-derived SST yields positive $\Delta\delta^{18}O_{sw}$ anomalies during glacials indicating elevated SSS. Warm SST and high $\Delta\delta^{18}O_{sw}$ at our core sites are indicative of a strengthened influence during glacial periods of warm saline Agulhas waters. This is strikingly different from the $U^{K'}_{37}$-derived SST record at the nearby CBR location [*Schneider et al.*, 1999; *Peeters et al.*, 2004] that displays accelerated warming only during the glacial Terminations while glacial SST are decreased with respect to interglacial levels. The different SST reconstructions possibly reflect on different living habitats and growth seasons of the alkenone producers and *G. bulloides* as the Mg/Ca signal carrier, in conjunction with seasonal variations of Agulhas

water transports and lateral shifts of the Agulhas retroflection. Meridional migrations of the STF, indicated by the planktonic foraminiferal STF index at the CBR location [*Peeters et al.*, 2004], likely exerted further control on warm and salt water transports through the Agulhas Corridor as it is reflected by the correlation between the STF index record and our SST and $\Delta\delta^{18}O_{sw}$ profiles. The offset pattern between the $U^{K'}_{37}$- and Mg/Ca-derived SST records cautions the interpretation of the proxy records as uniquely reflecting the hydrography of the Agulhas Current and Leakage and warrants an improved dynamical understanding of the interocean water exchange under contrasting climates of the present and past.

[32] **Acknowledgments.** We thank the International Marine Global Change Studies (IMAGES) project and the Institut Polaire Francais Paul Emile Victor (IPEV) for technical support and for making the R/V *Marion Dufresne* available for core retrieval. For their laboratory assistance with the stable isotope and trace element analyses we are indebted to H. Medley (Cardiff) and J. Perona and T. Padró (Serveis Científic Tècnics, Universitat de Barcelona). We thank Ule Ninnemann and an anonymous reviewer for their constructive comments which helped improve this manuscript. R.Z., G.M.M., and C.N. acknowledge support from the Ministerio de Educación y Ciencia, Spain (grants REN2002-01958, CGL2007-61579/CLI, BES2003-1530); I.C., R.Z., and L.D.P. received support the Comer Abrupt Climate Change Foundation (USA); and I.H. acknowledges support by the Natural Environment Research Council (NERC). We are also grateful to the NOSAMS facility at the Wood Hole Oceanographic Institution for the ^{14}C dates of core MD02-2594.

References

Bard, E. (2001), Comparison of alkenone estimates with other paleotemperature proxies, *Geochem. Geophys. Geosyst.*, *2*, 1002, doi:10.1029/2000GC000050.

Bard, E., and R. E. M. Rickaby (2009), Migration of the subtropical front as a modulator of glacial climate, *Nature*, *460*, 380–383, doi:10.1038/nature08189.

Barker, S., M. Greaves, and H. Elderfield (2003), A study of cleaning procedures used for foraminiferal Mg/Ca paleothermometry, *Geochem. Geophys. Geosyst.*, *4*(9), 8407, doi:10.1029/2003GC000559.

Bemis, B. E., H. Spero, J. Bijma, and D. W. Lea (1998), Reevaluation of the oxygen isotopic composition of planktonic foraminifera: Experimental results and revised paleotemperature equations, *Paleoceanography*, *13*, 150–160, doi:10.1029/98PA00070.

Bemis, B. E., H. J. Spero, and R. C. Thunell (2002), Using species-specific paleotemperature equations with foraminifera: A case study in the Southern California Bight, *Mar. Micropaleontol.*, *46*, 405–430, doi:10.1016/S0377-8398(02)00083-X.

Bertrand, P., et al. (1997), Les rapport de campagne à la mer à bord du Marion Dufresne—Campagne NAUSICAA—Images II—MD105 du 20/10/96 au 25/11/96, Inst. Fr. pour la Rech. et la Technol. Polaires, Plouzané, France.

Biastoch, A., C. W. Böning, and J. R. E. Lutjeharms (2008), Agulhas leakage dynamics affects decadal variability in Atlantic overturning circulation, *Nature*, *456*, 489–492, doi:10.1038/nature07426.

Biastoch, A., C. W. Böning, F. U. Schwarzkopf, and J. R. E. Lutjeharms (2009), Increase in Agulhas leakage due to poleward shift of Southern Hemisphere westerlies, *Nature*, *462*, 495–498, doi:10.1038/nature08519.

Bigg, G. R., and E. J. Rohling (2000), An oxygen isotope data set for marine waters, *J. Geophys. Res.*, *105*, 8527–8535, doi:10.1029/2000JC900005.

Boyle, E. A. (1983), Manganese carbonate overgrowths on foraminifera tests, *Geochim. Cosmochim. Acta*, *47*, 1815–1819, doi:10.1016/0016-7037(83)90029-7.

Boyle, E. A., and Y. Rosenthal (1996), Chemical Hydrography of the South Atlantic during the Last Glacial Maximum: Cd *vs* $\delta^{13}C$, in *The South Atlantic: Present, Past and Future*, edited by G. Wefer et al., pp. 423–443, Springer, Berlin.

Brathauer, U., and A. Abelmann (1999), Late Quaternary variations in sea surface temperatures and their relationship to orbital forcing recorded in the Southern Ocean (Atlantic sector), *Paleoceanography*, *14*, 135–148, doi:10.1029/1998PA900020.

Chang, Y.-P., C.-C. Chang, L.-W. Wang, M.-T. Chen, C.-H. Wang, and E.-F. Yu (1999), Planktonic foraminiferal sea surface temperature variations in the southeast Atlantic Ocean: A high-resolution record MD96-2085 of the past 400,000 years from the IMAGES II-NAUSICAA cruise, *Tao*, *10*, 185–200.

Conte, M. H., M.-A. Sicre, C. Rühlemann, J. C. Weber, S. Schulte, D. Schulz-Bull, and T. Blanz (2006), Global temperature calibration of the alkenone unsaturation index ($U^{K'}_{37}$) in surface waters and comparison with surface sediments, *Geochem. Geophys. Geosyst.*, *7*, Q02005, doi:10.1029/2005GC001054.

Cortese, G., A. Abelmann, and R. Gersonde (2007), The last five glacial-interglacial transitions: A high-resolution 450,000-year record from the subantarctic Atlantic, *Paleoceanography*, *22*, PA4203, doi:10.1029/2007PA001457.

de Ruijter, W. P. M., A. Biastoch, S. S. Drijfhout, J. R. E. Lutjeharms, R. P. Matano, T. Pichevin, P. J. van Leeuwen, and W. Weijer (1999), Indian-Atlantic interocean exchange: Dynamics, estimations and impact, *J. Geophys. Res.*, *104*, 20,885–20,910, doi:10.1029/1998JC900099.

Dickson, A. J., M. J. Leng, M. A. Maslin, H. J. Sloane, J. Green, J. A. Bendle, E. L. McClymont, and R. D. Pancost (2010), Atlantic overturning circulation and Agulhas leakage influences on southeast Atlantic upper ocean hydrography during marine isotope stage 11, *Paleoceanography*, *25*, PA3208, doi:10.1029/2009PA001830.

Dueñas-Bohórquez, A., R. E. da Rocha, A. Kuroyanagi, J. Bijma, and G. J. Reichart (2009), Effect of salinity and seawater calcite saturation state on Mg and Sr incorporation in cultured planktonic foraminifera, *Mar. Micropaleontol.*, *73*, 178–189, doi:10.1016/j.marmicro.2009.09.002.

Elderfield, H., and G. Ganssen (2000), Past temperature and $\delta^{18}O$ of surface ocean waters inferred from foraminiferal Mg/Ca ratios, *Nature*, *405*, 442–445, doi:10.1038/35013033.

Fairbanks, R. G., R. A. Mortlock, T.-C. Chiu, L. Cao, A. Kaplan, T. P. Guilderson, T. W. Fairbanks, A. L. Bloom, P. M. Grootes, and M.-J. Nadeau (2005), Radiocarbon calibration curve spanning 0 to 50,000 years BP based on paired $^{230}Th/^{234}U/^{238}U$ and ^{14}C dates on pristine corals, *Quat. Sci. Rev.*, *24*, 1781–1796, doi:10.1016/j.quascirev.2005.04.007.

Ferguson, J. E., G. M. Henderson, M. Kucera, and R. E. M. Rickaby (2008), Systematic change of foraminiferal Mg/Ca ratios across a strong salinity gradient, *Earth Planet. Sci. Lett.*, *265*, 153–166, doi:10.1016/j.epsl.2007.10.011.

Feron, R. C. V., W. P. M. de Ruijter, and D. Oskan (1992), Ring shedding in the Agulhas Current system, *J. Geophys. Res.*, *97*(9), 9467–9477, doi:10.1029/92JC00736.

Flores, J. A., R. Gersonde, and F. J. Sierro (1999), Pleistocene fluctuations in the Agulhas Current retroflection based on the calcareous plankton record, *Mar. Micropaleontol.*, *37*, 1–22, doi:10.1016/S0377-8398(99)00012-2.

Fraile, I., S. Mulitza, and M. Schulz (2009), Modeling planktonic foraminiferal seasonality: Implications for sea-surface temperature reconstructions, *Mar. Micropaleontol.*, *72*, 1–9, doi:10.1016/j.marmicro.2009.01.003.

Franzese, A. M., S. R. Hemming, S. L. Goldstein, and R. F. Anderson (2006), Reduced Agulhas leakage during the Last Glacial Maximum inferred from an integrated provenance and flux study, *Earth Planet. Sci. Lett.*, *250*, 72–88, doi:10.1016/j.epsl.2006.07.002.

Franzese, A. M., S. R. Hemming, and S. L. Goldstein (2009), Use of strontium isotopes in detrital sediments to constrain the glacial position of the Agulhas Retroflection, *Paleoceanography*, *24*, PA2217, doi:10.1029/2008PA001706.

Ganssen, G., and D. Kroon (2000), The isotopic signature of planktonic foraminifera from NE Atlantic surface sediments: Implications for the reconstruction of past oceanic conditions, *J. Geol. Soc.*, *157*, 693–699, doi:10.1144/jgs.157.3.693.

Gersonde, R., et al. (2003), Last glacial sea surface temperatures and sea-ice extent in the Southern Ocean (Atlantic-Indian sector): A multiproxy approach, *Paleoceanography*, *18* (3), 1061, doi:10.1029/2002PA000809.

Gersonde, R., X. Crosta, A. Abelmann, and L. Armand (2005), Sea-surface temperature and sea ice distribution of the Southern Ocean at the epilog Last Glacial Maximum—A circum-Antarctic view based on siliceous microfossil records, *Quat. Sci. Rev.*, *24*, 869–896, doi:10.1016/j.quascirev.2004.07.015.

Giraudeau, J., Y. Balut, I. R. Hall, A. Mazaud, and R. Zahn (2003), SWAF-MD128 Scientific Report, *Rep. OCE/2003/01*, 108 pp., Inst. Polaire Fr., Plouzané, France.

Gordon, A. L. (2003), The brawniest retroflection, *Nature*, *421*, 904–905, doi:10.1038/421904a.

Groeneveld, J., D. Nürnberg, R. Tiedemann, G.-J. Reichart, S. Steph, L. Reuning, D. Crudeli, and P. Mason (2008), Foraminiferal Mg/Ca increase in the Caribbean during the Pliocene: Western Atlantic Warm Pool formation, salinity influence, or diagenetic overprint?, *Geochem. Geophys. Geosyst.*, *9*, Q01P23, doi:10.1029/2006GC001564.

Hut, G. (1987), Consultants' Group Meeting on Stable Isotope Reference Samples for Geochemical and Hydrological Investigations, report to the Director General, pp. 1–42, Int. At. Agency, Vienna.

Kiefer, T., I. N. McCave, and H. Elderfield (2006), Antarctic control on tropical Indian Ocean sea surface temperature and hydrography, *Geophys. Res. Lett.*, *33*, L24612, doi:10.1029/2006GL027097.

Kısakürek, B., A. Eisenhauer, F. Böhm, D. Garbe-Schönberg, and J. Erez (2008), Controls on shell Mg/Ca and Sr/Ca in cultured planktonic foraminiferan, *Globigerinoides ruber* (white), *Earth Planet. Sci. Lett.*, *273*, 260–269, doi:10.1016/j.epsl.2008.06.026.

Knorr, G., and G. Lohmann (2003), Southern Ocean origin for the resumption of Atlantic thermohaline circulation during deglaciation, *Nature*, *424*, 532–536, doi:10.1038/nature01855.

Knorr, G., and G. Lohmann (2007), Rapid transitions in the Atlantic thermohaline circulation triggered by global warming and meltwater during the last deglaciation, *Geochem. Geophys. Geosyst.*, *8*, Q12006, doi:10.1029/2007GC001604.

Lea, D., T. A. Maschiotta, and H. J. Spero (1999), Controls on magnesium and strontium uptake in planktonic foraminifera determined by live culturing, *Geochim. Cosmochim. Acta*, *63*, 2369–2379, doi:10.1016/S0016-7037(99)00197-0.

Levi, C., et al. (2007), Low-latitude hydrological cycle and rapid climate changes during the last deglaciation, *Geochem. Geophys. Geosyst.*, *8*, Q05N12, doi:10.1029/2006GC001514.

Lutjeharms, J. R. E. (1996), The exchange of water between the South Indian and the South Atlantic, in *The South Atlantic: Present and Past Circulation*, edited by W. H. B. G. Wefer, G. Siedler, and D. Webb, pp. 125–162, Springer, Berlin.

Lutjeharms, J. R. E. (2006), *The Agulhas Current*, 329 pp., Springer, Berlin.

Martínez-Méndez, G., R. Zahn, I. R. Hall, L. D. Pena, and I. Cacho (2008), 345,000-year-long multi-proxy records off South Africa document variable contributions of Northern versus Southern Component Water to the deep South Atlantic, *Earth Planet. Sci. Lett.*, *267*, 309–321, doi:10.1016/j.epsl.2007.11.050.

Martínez-Méndez, G., E. G. Molyneux, R. Zahn, and I. R. Hall (2009), Variation in the glacial to interglacial water column structure of the Southern Ocean, *Quat. Sci. Rev.*, *28*, 3379–3387, doi:10.1016/j.quascirev.2009.09.022.

Mashiotta, T. A., D. W. Lea, and H. J. Spero (1999), Glacial-interglacial changes in subantarctic sea surface temperature and δ^{18}O-water using foraminiferal Mg, *Earth Planet. Sci. Lett.*, *170*, 417–432, doi:10.1016/S0012-821X(99)00116-8.

Matano, R. P., C. G. Simionato, W. P. de Ruijter, P. J. van Leeuween, P. T. Strub, D. B. Chelton, and M. Schlax (1998), Seasonal variability in the Agulhas Retroflection region, *Geophys. Res. Lett.*, *25*, 4361–4364, doi:10.1029/1998GL900163.

Matano, R. P., C. G. Simionato, and P. T. Strub (1999), Modeling the wind-driven variability of the south Indian Ocean, *J. Phys. Oceanogr.*, *29*, 217–230, doi:10.1175/1520-0485(1999)029<0217:MTWDVO>2.0.CO;2.

Mollenhauer, G., T. I. Eglinton, R. R. Schneider, P. J. Müller, P. M. Grootes, and J. Rullkötter (2003), Asynchronous alkenone and foraminifera records from the Benguela Upwelling System, *Geochim. Cosmochim. Acta*, *67*, 2157–2171, doi:10.1016/S0016-7037(03)00168-6.

Negre, C., R. Zahn, A. L. Thomas, P. Masqué, G. M. Henderson, G. Martínez-Méndez, I. R. Hall, and J. L. Mas (2010), Reversed Atlantic Deep Water flow during the Last Glacial Maximum, *Nature*, *468*, 84–88, doi:10.1038/nature09508.

Niebler, H. S., H. W. Hubberten, and R. Gersonde (1999), Oxygen isotope values of planktonic foraminifera: A tool for the reconstruction of surface water stratification, in *Use of Proxies in Paleoceanography: Examples From the South Atlantic*, edited by G. Fischer and G. Wefer, pp. 165–189, Springer, Berlin.

Nürnberg, D., J. Bijma, and C. Hemleben (1996), Assessing the reliability of magnesium in foraminiferal calcite as a proxy for water mass temperatures, *Geochim. Cosmochim. Acta*, *60*, 803–814, doi:10.1016/0016-7037(95)00446-7.

Pahnke, K., and R. Zahn (2005), Southern Hemisphere water mass conversion linked with North Atlantic climate variability, *Science*, *307*, 1741–1746, doi:10.1126/science.1102163.

Pahnke, K., R. Zahn, H. Elderfield, and M. Schulz (2003), 340,000-year centennial-scale marine record of Southern Hemisphere climatic oscillation, *Science*, *301*, 948–952, doi:10.1126/science.1084451.

Peeters, F. J. C., R. Acheson, G.-J. A. Brummer, W. P. M. de Ruijter, R. Schneider, G. Ganssen, M. E. Ufkes, and D. Kroon (2004), Vigorous exchange between the Indian and Atlantic Oceans at the end of the past five glacial periods, *Nature*, *430*, 661–665, doi:10.1038/nature02785.

Pena, L., E. Calvo, I. Cacho, S. Eggins, and C. Pelejero (2005), Identification and removal of Mn-Mg-rich contaminant phases on foraminiferal tests: Implications for Mg/Ca Past temperature reconstructions, *Geochem. Geophys. Geosyst.*, *6*, Q09P02, doi:10.1029/2005GC000930.

Prahl, F. G., A. C. Mix, and M. A. Sparrow (2006), Alkenone paleothermometry: Biological lessons from marine sediment records off western South America, *Geochim. Cosmochim. Acta*, *70*, 101–117, doi:10.1016/j.gca.2005.08.023.

Rau, A. J., J. Rogers, J. R. E. Lutjeharms, J. Giraudeau, J. A. Lee-Thorp, M.-T. Chen, and C. Waelbroeck (2002), A 450-kyr record of hydrological conditions on the western Agulhas Bank Slope, south of Africa, *Mar. Geol.*, *180*, 183–201, doi:10.1016/S0025-3227(01)00213-4.

Rau, A. J., J. Rogers, and M.-T. Chen (2006), Late Quaternary palaeoceanographic record in giant piston cores off South Africa, possibly including evidence of neotectonism, *Quat. Int.*, *148*, 65–77, doi:10.1016/j.quaint.2005.11.007.

Regenberg, M., D. Nürnberg, S. Steph, J. Groeneveld, D. Garbe-Schönberg, R. Tiedemann, and W.-C. Dullo (2006), Assessing the effect of dissolution on planktonic foraminiferal Mg/Ca ratios: Evidence from Caribbean core tops, *Geochem. Geophys. Geosyst.*, *7*, Q07P15, doi:10.1029/2005GC001019.

Rosenthal, Y., G. P. Lohman, K. C. Lohman, and R. M. Sherrell (2000), Incorporation and preservation of Mg in *Globigerinoides Sacculifer*: Implications for reconstructing the temperature and $^{18}O/^{16}O$ of seawater, *Paleoceanography*, *15*, 135–145, doi:10.1029/1999PA000415.

Sadekov, A. Y., S. M. Eggins, P. De Deckker, U. Ninnemann, W. Kuhnt, and F. Bassinot (2009), Surface and subsurface seawater temperature reconstruction using Mg/Ca microanalysis of planktonic foraminifera *Globigerinoides ruber, Globigerinoides sacculifer*, and *Pulleniatina obliquiloculata*, *Paleoceanography*, *24*, PA3201, doi:10.1029/2008PA001664.

Saher, M. H., F. Rostek, S. J. A. Jung, E. Bard, R. R. Schneider, M. Greaves, G. M. Ganssen, H. Elderfield, and D. Kroon (2009), Western Arabian sea SST during the penultimate interglacial: A comparison of $U^{K'}_{37}$ and Mg/Ca paleothermometry, *Paleoceanography*, *24*, PA2212, doi:10.1029/2007PA001557.

Schneider, R. R., P. J. Müller, and R. Acheson (1999), Atlantic alkenone sea-surface temperature records: Low versus mid latitudes and differences between hemispheres, in *Reconstructing Ocean History: A Window Into the Future*, edited by F. Abrantes and A. C. Mix, pp. 33–55, Plenum, New York.

Schrag, D. P., J. F. Adkins, K. McIntyre, J. L. Alexander, D. A. Hodell, C. D. Charles, and J. F. McManus (2002), The oxygen isotopic composition of seawater during the Last Glacial Maximum, *Quat. Sci. Rev.*, *21*, 331–342, doi:10.1016/S0277-3791(01)00110-X.

Siddall, M., E. J. Rohling, A. Almogi-Labin, C. Hemleben, D. Meischner, I. Schmelzer, and D. A. Smeed (2003), Sea-level fluctuations during the last glacial cycle, *Nature*, *423*, 853–858, doi:10.1038/nature01690.

Sikes, E. L., T. O'Leary, S. D. Nodder, and J. K. Volkman (2005), Alkenone temperature records and biomarker flux at the subtropical front on the Chatham Rise, SW Pacific Ocean, *Deep Sea Res., Part I*, *52*, 721–748, doi:10.1016/j.dsr.2004.12.003.

Southon, J., M. Kashgarian, M. Fontugne, B. Metivier, and W. W.-S. Yim (2002), Marine reservoir corrections for the Indian Ocean and Southeast Asia, *Radiocarbon*, *44*, 167–180.

Tyson, P. D. (1986), *Climate Change and Variability in Southern Africa*, 220 pp., Oxford Univ. Press, Cape Town, South Africa.

van Sebille, E., A. Biastoch, P. J. van Leeuwen, and W. P. M. de Ruijter (2009), A weaker Agulhas Current leads to more Agulhas leakage, *Geophys. Res. Lett.*, *36*, L03601, doi:10.1029/2008GL036614.

Visser, K., R. Thunell, and L. Stott (2003), Magnitude and timing of temperature change in the Indo-Pacific Warm Pool during deglaciation, *Nature*, *421*, 152–155, doi:10.1038/nature01297.

Volbers, A. N. A., and R. Henrich (2002), Late Quaternary variations in calcium carbonate preservation of deep-sea sediments in the northern Cape Basin: Results from a multiproxy approach, *Mar. Geol.*, *180*, 203–220, doi:10.1016/S0025-3227(01)00214-6.

Volbers, A. N. A., and R. Henrich (2004), Calcium carbonate corrosiveness in the South Atlantic during the Last Glacial Maximum as inferred from changes in the preservation of *Globigerina bulloides*: A proxy to determine deep-water circulation patterns?, *Mar. Geol.*, *204*, 43–57, doi:10.1016/S0025-3227(03)00372-4.

Waelbroeck, C., L. Labeyrie, E. Michel, J.-C. Duplessy, J. F. McManus, K. Lambeck, E.

Balbon, and M. Labracherie (2002), Sea-level deep water temperature changes derived from benthic foraminifera isotopic records, *Quat. Sci. Rev.*, *21*, 295–305, doi:10.1016/S0277-3791(01)00101-9.

I. Cacho, GRC Geociències Marines, Departament d'Estratigrafia, Paleontologia i Geociències Marines, Universitat de Barcelona, C/Martí i Franquès, s/n, E-08028 Barcelona, Spain.

I. R. Hall, School of Earth and Ocean Sciences, Cardiff University, Main Building, Park Place, Cardiff CF10 3YE, UK.

G. Martínez-Méndez, Center for Marine Environmental Sciences (MARUM), University of Bremen, Leobener Str., D-28359 Bremen, Germany. (gmartinez@marum.de)

C. Negre, Centre d'Innovació i Formació Ocupacional Santa Coloma, Departament de Treball, Generalitat de Catalunya, Ramon Berenguer IV s/n, E-08924 Santa Coloma de Gramenet, Spain.

F. J. C. Peeters, Section Marine Biogeology, Faculty of Earth and Life Sciences, VU University Amsterdam, de Boelelaan 1085, NL-1081 HV Amsterdam, Netherlands.

L. D. Pena, Lamont-Doherty Earth Observatory, 61 Rt. 9W, Palisades, NY 10964, USA.

R. Zahn, Institut de Ciència i Tecnologia Ambientals, Universitat Autònoma de Barcelona, Edifici Cn Campus UAB, E-08193 Bellaterra, Spain. (rainer.zahn@uab.cat)